Microfluid Nanofluid (2010) 9:973–979
DOI 10.1007/s10404-010-0598-z

SHORT COMMUNICATION

Concentration-enhanced rapid detection of human chorionic gonadotropin as a tumor marker using a nanofluidic preconcentrator

Jeong Hoon Lee · Jongyoon Han

Received: 12 January 2010 / Accepted: 10 March 2010 / Published online: 30 March 2010

Abstract Here, we report a new method of concentration-enhanced binding kinetics for a rapid immunoassay screening test on a gold surface in a poly(dimethylsiloxane) (PDMS) microfluidic chip format. The use of alkylthiolate self-assembled monolayers on gold surfaces of a PDMS-glass microchip resulted in accelerated binding kinetics at an electrokinetic trapping zone. We used human chorionic gonadotropin (hCG) as a model analyte for a tumor marker to demonstrate the potential ability of dynamic preconcentrating operation in serum using 1D planar gold surface and demonstrated concentration-enhanced binding kinetics by 500-fold. The preconcentration of cy3 labeled streptavidin onto biotinylated Au surface also revealed that the binding kinetics of the protein were linearly proportional to the concentration profile of the preconcentration plug. We showed rapid detection of hCG in the clinical range with a shorten total assay time of 15 min. The enhanced binding kinetics between hCG antigen-antibody via preconcentration showed good feasibility for use in a rapid immunoassay screening test.

Keywords Microfluidic · Nanofluidic · HCG tumor marker · Preconcentrator · Rapid immunoassays

J. H. Lee
Department of Electrical Engineering, Kwangwoon University, 447-1, Wolgye, Nowon, Seoul 139-701, South Korea

J. Han (✉)
Departments of Electrical Engineering and Computer Science, and Biological Engineering, Massachusetts Institute of Technology, Cambridge, MA 02139, USA
e-mail: jyhan@mit.edu

1 Introduction

To detect a low abundance of biomolecules, such as biomarkers in a complex proteomic samples, many advanced immunoassay have been developed, including SPR, nanowire sensors, nanoparticle based assays and nanomechanical sensors (Cui et al. 2001; Kukanskis et al. 1999; Lee et al. 2005). Physiological fluids such as serum contain numerous soluble proteins that spontaneously react with solid surfaces in very dynamic ways (Andrade 1985). To minimize complex competition among over 200 proteins, several different surface chemistries on variable materials (e.g., polyurethanes, silicones, metal alloys) have been suggested. Among the materials clinically applied for the receptor surfaces of immunosensors, self-assembled monolayers (SAMs) on gold substrates are widely used and have been shown to yield the most well-ordered, homogeneous monolayers with controlled surface chemistry for DNA, protein and small molecule biosensors (Canaria et al. 2006; Dubois and Nuzzo 1992; Kukanskis et al. 1999; Ulman 1991). Alkylthiols SAMs on gold substrates have been the most widely used and has been shown to provide a very stable surface for immunosensors (Badia et al. 1997; Gong et al. 2006; Lang et al. 1999).

Previous studies have shown that the 1D planar sensor (Au surface) has a diffusion limited transport of $\sim t^{1/2}$, while the 2D sensor (nanowire) and 3D sensor (nanosphere) have a diffusion limited transport of $\sim t^{1}$, consequently, the 1D sensor has a more limited response time to capture analyte molecules relative to the 2D and 3D sensors (Nair and Alam 2006). However, alkylthiols SAMs on gold substrates is still a well-engineered surface for commercial biosensors. Moreover, one can directly utilize Au surfaces as the electric detection platform for QCM, cantilevers and nanosensors.

Our group recently developed novel nanofluidic biomolecule concentration devices that can be used to collect and trap proteins contained in a given sample into a much smaller volume, thereby significantly increasing the local concentration (Lee et al. 2007, 2008; Wang et al. 2005). This device can take a sample volume of 1–25 μl and continuously collect/trap any charged biomolecules, such as proteins, until a sufficient amount of the sample is collected in a very small volume (1 pl to 1 nl). More recently, we demonstrated that the pre-binding sensitivity could be enhanced by more than 500-fold when a charge-based silicon-based nanofluidic biomolecule preconcentrator was combined with a bead-based immunoassay (Wang and Han 2008). However, the operation of the device was only demonstrated with a 10 mM dibasic phosphate buffer solution since the 40 nm channel depth was not large enough for operation in a high buffer concentration.

In this study, we introduced a new method to increase the pre-binding concentration by combining a polymer-based nanofluidic preconcentrator with a 1D planar Au sensor, thereby increasing the local sensor area and consequently enhancing the limit of detection and shortening the assay time. Using this approach, the electrokinetic device could be operated using a phosphate buffered saline solution (1× PBS; 137 mM NaCl, 2.7 mM KCl, 10 mM, pH ~7.4).

To test the feasibility of this assay, we used human chorionic gonadotropin (hCG) as a model tumor marker as well as the well-characterised streptavidin–biotin interaction (Weber et al. 1989). The detection and measurement of hCG has been generally used in early pregnancy testing. Also, hCG is an important tumor marker since the human chorionic gonadotropin is also secreted by some cancers including choriocarcinoma, germ cell tumors, hydatidiform mole formation, trophoblastic disease and testicular cancer (Cole 1997; Kurman et al. 1977; Mock et al. 2000; Moulton et al. 2002). For the testicular cancer detection, different hCG levels in men were reported as clinically relevant, in various sample conditions and situations (Cole 1997; Lempiainen et al. 2008; Mann and Karl 1983). For the serum tests, a chemiluminescent or fluorimetric immunoassay has been commercially used with a serum sample of 20 μl (Autobio Diagnostics Co. Ltd.) and 50 μl (e.g. Diagnostic Automation, Inc.) and reported assay time was >1 h since they required incubation time.

Herein, we report that this concentration-enhanced rapid detection immunoassay was able to detect hCG for testicular cancer and trophoblastic disease (1 IU/ml, converted from 100 ng/ml (2.72 nM) by supplier's data sheet) within a shorten total assay time of 15 min (10 min preconcentration, 5 min washing/drying and measurement step).

2 Experimental

2.1 Chip design and fabrication

The PDMS preconcentrator with both the surface-patterned Nafion membrane (for permselective nanochannel) and Au dot arrays (for immunoassay) on the glass substrate is shown in Fig. 1. We designed the microchannel network with the assay area (12 μm deep and 70 μm wide; in Fig. 1b) as well as the damper channel (12 μm deep, 20 μm wide and 1 mm long) to reduce the pressure drop during the dynamic preconcentration operation; in Fig. 1c). For the 1D planar Au sensor, Au dot arrays with 20 μm diameter were prepared on 4″ glass wafer (Wafernet, Inc. CA). After completion of the lift-off process using standard photolithography, a 200 nm thick Au was deposited using an e-beam evaporator (Temescal VES2550) with 30 nm chrome layer for adhesion on the glass substrate (see Fig. 1b). Then, the glass wafer was coated with a 1 μm thick photoresist without baking to prevent particle contamination of the Au surface during the die-saw process. After the dicing process, the unit glass chip was thoroughly cleaned with acetone, methanol, piranha (H_2SO_4:H_2O_2 = 3:1) and DI water to remove dicing particles and photoresist before Nafion® printing.

Nafion® is a well-known ionomer with high ionic permselectivity due to cluster networks as well as sulfonate groups (Roche et al. 1981). Due to high ionic permselectivity, Nafion® with 190 nm thick patterned on glass functions the nanofluidic channel. Magnified images of the PDMS preconcentrator after plasma bonding between the PDMS microchannel and glass with Nafion and 1D Au dot arrays are shown in Fig. 1b. For Nafion® printing on the area between the Au dot arrays, a microflow patterning technique, which utilizes the PDMS microchannel (reversibly bonded to glass; 120 μm deep and 200 μm wide), was applied to define the ion-selective nanobridge (Lee et al. 2008). After placing a drop of liquid Nafion® resin (1 μl) at one open reservoir on the channel, a negative pressure was applied at other open reservoir. A capillary force induced ion-selective film was formed that was 190 nm thick. The film was then cured by incubation at 95°C for 10 min. The small pore size and charge density of Nafion® enabled the PDMS preconcentrator to operate when using a common assay solution (1× PBS; relatively high ionic concentration condition), which normally does not occur for Si-based preconcentrators with 40 nm deep nanochannels (Wang and Han 2008).

2.2 Chip operation and immunoassay

To test the operation of the device in concentrating-enhanced immunoassays (see Fig. 1d), the middle channel

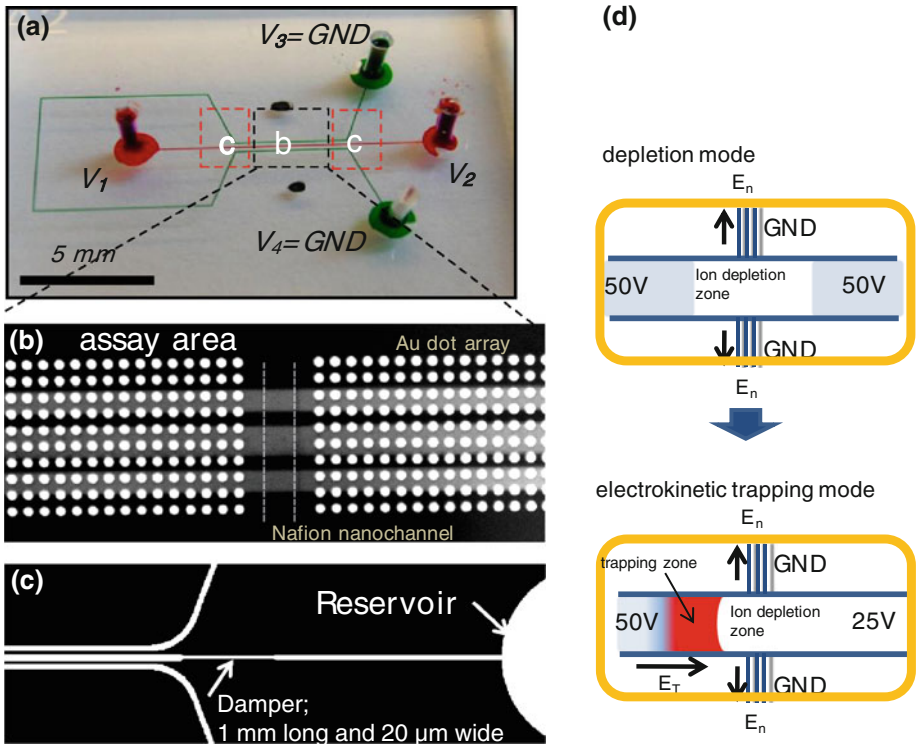

Fig. 1 **a** Schematic of the PDMS preconcentrator with the surface-patterned Nafion membrane on the glass substrate and its operation. **b** Au dot arrays (diameter = 20 μm) on the glass slide for the immunoassay application. The middle channel is loaded with a hCG protein (in 1× PBS) and the side channel is filled with a 1× PBS buffer solution. **c** Damper design for reducing the pressure difference between the two reservoirs. **d** For preconcentration, a potential difference was applied across the middle and the side channel in combination with an electrokinetic flow. All the microchannels were 12 μm deep and 70 μm wide

was loaded with a protein (case 1; streptavidin in Fig. 3, case 2; hCG protein in Fig. 4) in 1× PBS; and the side channel was filled with a 1× PBS buffer solution. The device was operated in the depletion and concentration mode, as shown in Fig. 1d). After generating the depletion region by applying a potential difference (e.g., 50 V) between the microchannels (sample channel and buffer channel) through the planar ion-selective membrane (depletion mode), a potential difference across the sample channel was applied to allow the molecules to move through electroosmotic flow. Biomolecules were trapped by the depletion force due to the nanofluidic concentration polarization effect (Kim et al. 2007).

2.3 Immobilization

Figure 2 shows the schematic steps used for the water-based hCG protein immobilization via the formation of alkylthiolate self-assembled monolayers on Au surfaces. We prepared two ethylene glycol modified alkylthiolates, Tri(ethylene glycol) dodecylthiol (TEG) and Biotinylated tri(ethylene glycol) dodecylthiol (BAT), using de-ionized water with 1% ethanol (Canaria et al. 2006). Since organic solvents such as ethanol, dimethyl sulfoxide and hexane cause swelling and consequently PDMS delamination, we purchased water-based TEG and BAT chemicals from ProChimia Surfaces and prepared stock solutions of 100 mM TEG and 100 mM BAT in ethanol. Using DI-water, we diluted the stock solution to 0.1 mM. It has been well-known that ethylene glycol incorporation reduces the non-specific binding of protein, bacteria, and cells to Au surface (Harder et al. 1998). As a first step, we mixed a solution with a volume ratio of BAT:TEG = 1:1. After filling the center microchannel for 2 h to completely form the monolayers, the channel was flushed out with 1 vol.% (v/o) ethanol in DI-water. For the binding of streptavidin, 10 μg/ml of streptavidin was injected into the center microchannel, which was then sequentially flushed out with PBS, PBS with Tween 20 and PBS after 1 h. After binding of biotinated monoclonal 10 μg/ml anti-hCG (Fitzgerald Inc, MA) for 1 h (Fig.2d), we carried out surface blocking using a bovine serum albumin (BSA; 1% in PBS) solution to prevent non-specific binding. With this 1D planar sensor scheme, we assayed 100 ng/ml hCG protein (Human Chorionic Gonadotropin (HCG), Fitzgerald Inc, MA) labeled with Alexa488.

3 Results and discussion

3.1 Streptavidin–biotin interaction

The concentration-enhanced rapid immunoassay results of the streptavidin–biotin interaction are shown in Fig. 3. The biotin–streptavidin system is regarded as the strongest noncovalent biological interaction known, having a dissociation constant (K_d) on the order of 4×10^{-14} M (Green 1990). A cy3 labeled streptavidin was used to interact with

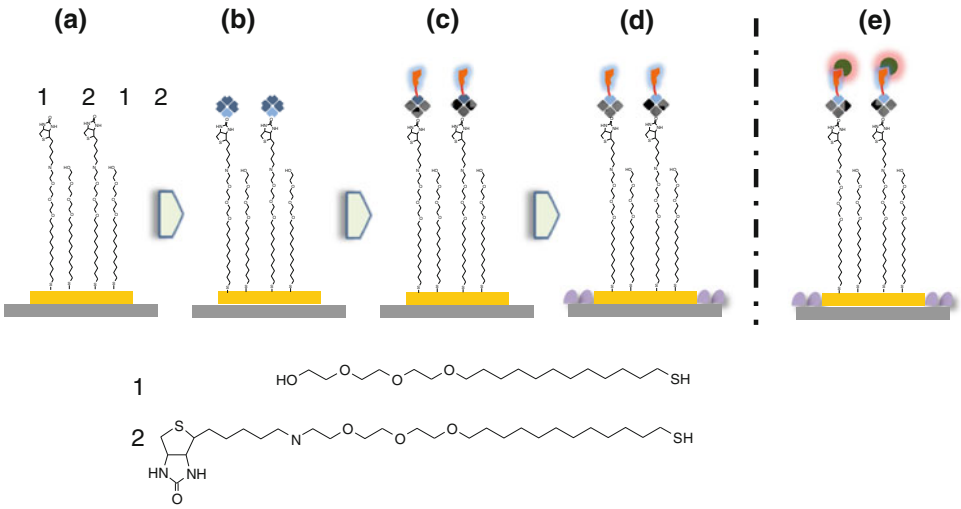

Fig. 2 Schematics of anti-hCG immobilization via the formation of alkylthiolate self-assembled monolayers on the Au surface. **a** Formation of Tri(ethylene glycol) dodecylthiol (TEG) and Biotinylated tri(ethylene glycol) dodecylthiol (BAT) on the Au surface. **b** Binding of streptavidin, **c** binding of biotinated monoclonal anti-hCG, **d** surface blocking using BSA (1% in PBS) for preventing non-specific binding. **e** Immunoassay using hCG protein labeled with Alexa488

a biotinylated Au surface. The on-site preconcentration step was conducted for 10 min with 100 ng/ml of streptavidin in 1× PBS. Since it has been reported that the dissociation constant (K_d) is 2–3 orders larger in a low target concentration environment than the when the reaction is saturated (de Mol et al. 2000), the time required for binding equilibrium to be reached will increase dramatically at lower antigen concentration (Wang and Han 2008).

The 10 min on-site concentrated fluorescence image and linear profile is shown in Fig. 3a. The measured profile along the microchannel after the 10 min on-site preconcentration step showed that the local concentration of cy3 labeled streptavidin was drastically increased in the concentrated reaction zone, indicated by the high-intensity plug in the fluorescence image and the corresponding intensity peak. After sequentially flushing out the microchannel with PBS, PBS with Tween 20, and PBS, the channel was dried completely and then the fluorescence intensity on the Au dot array was measured. Interestingly, the assay results taken from fluorescence intensity of the Au dot array showed dramatically improved binding kinetics in the preconcentration zone (Fig. 3b). The fluorescence images along the 5 points of the Au dot arrays (Fig. 3b) exactly correspond with the 10 min on-time preconcentration profile (Fig. 3a). To verify the specificity of the reaction, the assay was repeated using 1 μg/ml β-Phycoerythrin (β-PE protein; MW 240 kDa and pI $\sim$ 4.3; Sigma-Aldrich, MO) instead of streptavidin and no interaction was observed between the β-PE protein and biotinated Au surface (image not shown).

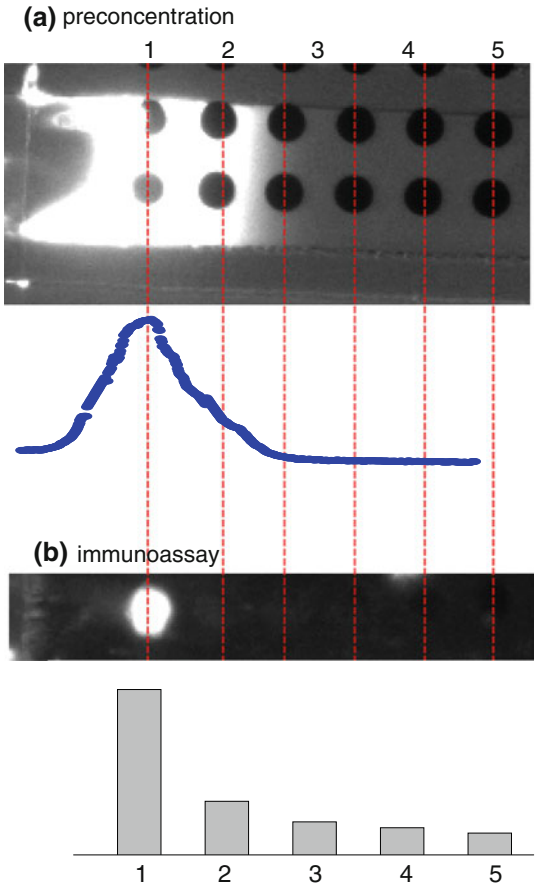

Fig. 3 **a** Preconcentration step using cy3 labeled streptavidin binding to a biotinlyated Au surface (after 10 min on-site preconcentration with 100 ng/ml streptavidin in 1× PBS). **b** Fluorescence image after washing the microchannel with the sequential injection of PBS, PBST(PBS with Tween20) and PBS. Fluorescence intensity of each Au dot indicates dramatically improved binding kinetics in the preconcentration zone

3.2 Immunoassay for hCG

hCG has been reported as an important tumor marker for choriocarcinoma, germ cell tumors, hydatidiform mole formation, and testicular cancer (Cole 1997; Kurman et al. 1977; Mock et al. 2000; Moulton et al. 2002); thus, there is a need to develop novel methods to detect hCG. The dissociation constant, K_d, of the hCG antibody was reported to

be 6.2 × 10^{-9} M based on the supplier's data sheet (http://www.fitzgerald-fii.com/uploadDocs/dataSheets/3463.pdf). When the target concentration was significantly below the K_d of the antibody, the interaction of the low-concentration target and the antibody is usually diffusion-limited (de Mol et al. 2000). As a result, a long reaction (incubation) time is typically required from several hours to overnight when using low concentration immunoassays (Cesaro-Tadic et al. 2004).

To verify the specificity of the interaction, the preconcentration operation was conducted with the β-PE protein in 1× PBS, 1 mg/ml of the BSA background protein and the biotinylated monoclonal anti-hCG immobilized Au dot array as shown in Fig. 4a. Fluorescence images were taken 10 min after the on-site preconcentrating operation and demonstrated that the operation was stable in 1× PBS solution. After washing the microchannel with PBS, PBS with Tween 20, and PBS, we confirmed that no non-specific binding events between immobilized anti-hCG and β-PE protein occurred (image not shown). To detect the specific binding event between anti-hCG and the hCG protein, the same 10 min on-site preconcentration step was conducted with 100 ng/ml of the hCG protein in a 1× PBS, 1 mg/ml of the BSA background protein and the biotinated monoclonal anti-hCG immobilized Au dot array. From the supplier's data sheet, 100 ng/ml of the hCG protein should be converted to 1 IU/ml. Since the hCG concentration (2.72 nM, 100 ng/ml) was below the K_d value of the hCG antibody (6.2 nM), the antigen–antibody (Ag–Ab) interaction was diffusion-limited, consequently, the reaction time could be quite long and last up to hours. Figure 4b shows the fluorescence image and intensity profile of electrokinetic trapping (taken after 10 min preconcentration). In addition, Fig. 4c shows the fluorescence image and intensity profile of hCG Ab–Ag interaction after the washing and drying step with a N_2 gun. The washing step was carried out with PBS, PBS with Tween 20, and PBS.

As observed for the biotin–streptavidin system, the Au dot arrays of hCG and anti-hCG binding event in the electrokinetic trapping zone displayed a significantly enhanced signal. The location of the preconcentration plug (4 bright dots in Fig. 4b) exactly corresponded with the 10 min on-time preconcentration profile (Fig. 4a). The fact that no significant increase in the fluorescence signal after 60 min of interaction between hCG and anti-hCG without the preconcentration step in the microchannel at same concentration (100 ng/ml hCG; data not shown) was observed demonstrates the distinct advantages of the on-site preconcentration device.

The enhanced sensitivity (Fig. 4c) as well as the preconcentration factor (Fig. 4b) was quantified using the reference fluorescence signal (50 µg/ml hCG; 500-fold higher concentration of assayed one). 50 µg/ml hCG was placed into the microchannel and the fluorescence intensity was measured without a preconcentration step after a 10 min interaction (linear dot profile in the graph of Fig. 4b). As shown in Fig. 4b, the sample concentration increased by at least 500-fold in 10 min. After the washing

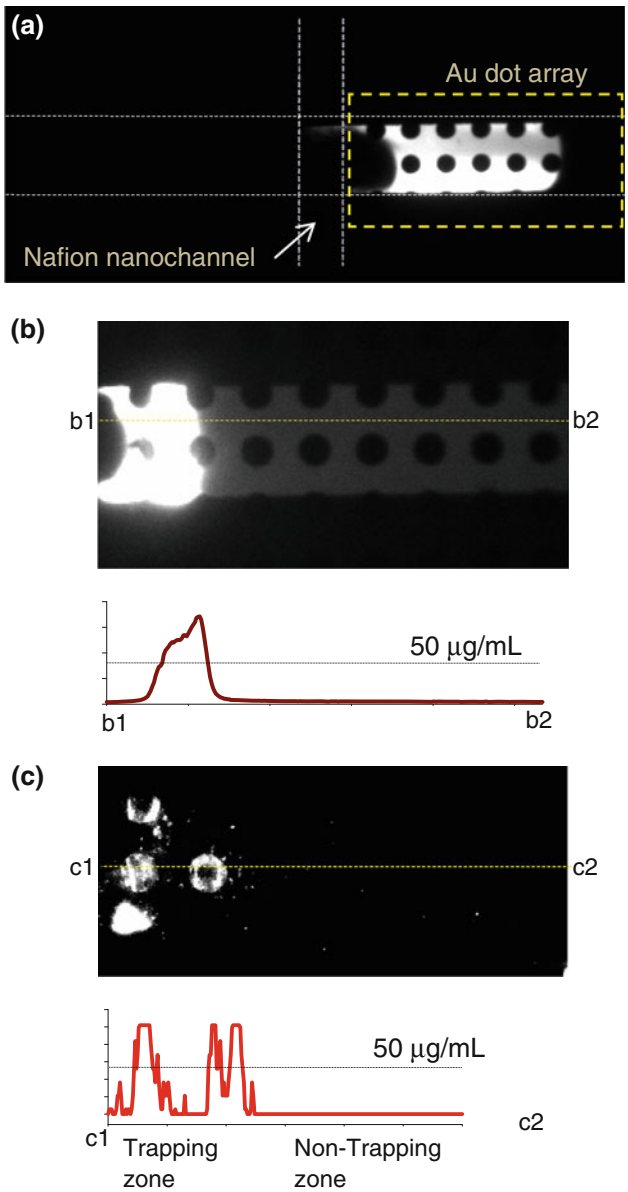

Fig. 4 **a** Stable operation of the preconcentration step (after 10 min, 1 µg/ml bBE in 1× PBS; with 1 mg/ml BSA background protein; V_1 = 50 V and V_2 = 25 V, V_3 = V_4 = GND in Fig. 1). No non-specific binding events between immobilized anti-hCG and bPE proteins were observed (image not shown). Magnified fluorescence image and intensity profile of **b** preconcentration of hCG protein (taken after 10 min preconcentration, 100 ng/ml hCG antigen in 1× PBS; with 1 mg/ml BSA background protein) and **c** fluorescence image and intensity profile after the washing and dry step of device **b**. These images demonstrate the enhanced binding kinetics between hCG Ag-Ab via preconcentration. From the reference intensity (hCG 50 µg/ml; *dot line*), a 500 fold increase in the sensitivity of the assay was observed

and dry step, we measured the line profile from the fluorescent signal. The line profile of the fluorescence signal indicated that the sensitivity of detecting bound protein on the Au surface was enhanced by 500-fold. In addition, we shorten the total assay time to 15 min, including preconcentration (10 min), washing/drying and measurement step (5 min). This binding kinetics follows the Langmuir isotherm $\theta = 1 - e^{-c(x)kt}$, where θ is the fraction of surface coverage of hCG, $c(x)$ is the protein concentration at position x, k is the reaction rate of the protein with the surface, and t is time. Evidently, one can expect that an increase in the local concentration at a constant binding time results in an increase in the fraction of surface coverage.

4 Conclusions

In this study, we developed a rapid pre-screen immunoassay method via concentration-enhanced binding kinetics. For the rapid immunoassay, we combined a simple disposable microfluidic chip format with alkylthiolate self-assembled monolayers on a 1D gold surface. By exploiting the high ionic permselectivity of Nafion®, which reduces the cluster network and the effective channel size and contains sulfonate groups, we demonstrated that this novel device could be stably operated in the high ionic concentrations of a PBS solution, and not in a dibasic buffer system ($\sim$10 mM). In addition, the total assay time for the detection of hCG for testicular cancer and trophoblastic disease was decreased to 15 min (10 min preconcentration, 5 min washing/drying and measurement step) with 25 μl sample volume. The enhanced binding kinetics between hCG Ag–Ab via preconcentration demonstrated that this technique holds great promise as a rapid immunoassay screening method for detection of small concentrations. Due to its sensitivity, we expect that it will be used as a pre-binding signal enhancement tool to detect low-abundance proteins and peptides. Furthermore, the PDMS microfluidic immunoassay format would allow for direct integration with many different biosensors using 1D Au surfaces that utilized post-binding amplification (i.e. QCM, cantilever and nanosensor).

Acknowledgments This work was supported by NIH (CA119402). J. H. Lee is partially supported by the Research Grant of Kwangwoon University in 2010.

References

Andrade J (1985) Surface and interfacial aspects of biomedical polymers. Pelnum Press, New York

Badia A, Demers L, Dickinson L, Morin FG, Lennox RB, Reven L (1997) Gold-sulfur interactions in alkylthiol self-assembled monolayers formed on gold nanoparticles studied by solid-state NMR. J Am Chem Soc 119(45):11104–11105

Canaria CA, So J, Maloney JR, Yu CJ, Smith JO, Roukes ML, Fraser SE, Lansford R (2006) Formation and removal of alkylthiolate self-assembled monolayers on gold in aqueous solutions. Lab Chip 6:289–295

Cesaro-Tadic S, Dernick G, Juncker D, Buurman G, Kropshofer H, Michel B, Fattinger C, Delamarche E (2004) High-sensitivity miniaturized immunoassays for tumor necrosis factor using microfluidic systems. Lab Chip 4:563–569

Cole LA (1997) Immunoassay of human chorionic gonadotropin, its free subunits, and metabolites. Clin Chem 43:2233–2243

Cui Y, Wei Q, Park H, Lieber CM (2001) Nanowire nanosensors for highly sensitive and selective detection of biological and chemical species. Science 293(5533):1289–1292

de Mol NJ, Plomp E, Fischer MJE, Ruijtenbeek R (2000) Kinetic analysis of the mass transport limited interaction between the tyrosine kinase lck SH2 domain and a phosphorylated peptide studied by a new cuvette-based surface plasmon resonance instrument. Anal Biochem 279(1):61–70

Dubois LH, Nuzzo RG (1992) Synthesis, structure and properties of model organic surfaces. Annu Rev Phys Chem 43:437–463

Gong P, Lee C-Y, Gamble LJ, Castner DG, Grainger DW (2006) Hybridization behavior of mixed DNA/alkylthiol monolayers on gold: characterization by surface plasmon resonance and 32P radiometric assay. Anal Chem 78:3326–3334

Green NM (1990) Avidin and streptavidin. Methods Enzymol 184:51–67

Harder P, Grunze M, Dahint R, Whitesides GM, Laibinis PE (1998) Molecular conformation in oligo(ethylene glycol)-terminated self-assembled monolayers on gold and silver surfaces determines their ability to resist protein adsorption. J Phys Chem B 102:426–436

Kim SJ, Wang Y-C, Lee JH, Jang H, Han J (2007) Concentration polarization and nonlinear electrokinetic flow near a nanofluidic channel. Phys Rev Lett 99:044501

Kukanskis K, Elkind J, Melendez J, Murphy T, Miller G, Garner H (1999) Anal Biochem 274:7–17

Kurman RJ, Scardino PT, McIntire KR, Waldmann TA, Javadpour N (1977) Cellular localization of alpha-fetoprotein and human chorionic gonadotropin in germ cell tumors of the testis using an indirect immunoperoxidase technique. A new approach to classification utilizing tumor markers. Cancer 40(5):2136–2151

Lang HP, Baller MK, Berger R, Gerberc C, Gimzewski JK, Battiston FM, Fornaro P, Ramseyer JP, Meyer E, Güntherodt HJ (1999) An artificial nose based on a micromechanical cantilever array. Anal Chim Acta 393(1–3):59–65

Lee JH, Hwang KS, Park J, Yoon KH, Yoon DS, Kim TS (2005) Immunoassay of prostate-specific antigen (PSA) using resonant frequency shift of piezoelectric nanomechanical microcantilever. Biosens Bioelectron 20(10):2157–2162

Lee JH, Chung S, Kim SJ, Han J (2007) Poly(dimethylsiloxane)-based protein preconcentration using a nanogap generated by junction gap breakdown. Anal Chem 79(17):6868–6873

Lee JH, Song Y-A, Han J (2008) Multiplexed proteomic sample preconcentration device using surface-patterned ion-selective membrane. Lab Chip 8(4):596–601

Lempiainen A, Stenman U-H, Blomqvist C, Hotakainen K (2008) Free {beta}-subunit of human chorionic gonadotropin in serum is a diagnostically sensitive marker of seminomatous testicular cancer. Clin Chem 54(11):1840–1843

Mann K, Karl H-J (1983) Molecular heterogeneity of human chorionic gonadotropin and its subunits in testicular cancer. Cancer 52(4):654–660

Mock P, Kovalevskaya G, O'Connor JF, Campana A (2000) Choriocarcinoma-like human chorionic gonadotrophin (HCG) and HCG bioactivity during the first trimester of pregnancy. Human Reprod 15(10):2209–2214

Moulton HM, Yoshihara PH, Mason DH, Iversen PL, Triozzi PL (2002) Active specific immunotherapy with a ß-human chorionic gonadotropin peptide vaccine in patients with metastatic colorectal cancer. Clin Cancer Res 8:2044–2051

Nair PR, Alam MA (2006) Performance limits of nanobiosensors. Appl Phys Lett 88:233120

Roche EJ, Pineri M, Duplessix R, Levelut AM (1981) J Polym Sci Polym Phys Ed 19:1

Ulman A (1991) An introduction to ultrathin organic films: from Langmuir-Blodgett to self-assembly. Academic Press, Boston

Wang Y-C, Han J (2008) Pre-binding dynamic range and sensitivity enhancement for immuno-sensors using nanofluidic preconcentrator. Lab Chip 8:392–394

Wang YC, Stevens AL, Han J (2005) Million-fold preconcentration of proteins and peptides by nanofluidic filter. Anal Chem 77:4293–4299

Weber PC, Ohlendorf DH, Wendoloski JJ, Salemme FR (1989) Structural origins of high-affinity biotin binding to streptavidin. Science 243(4887):85–88